

Regional climate simulations over the continental United States during the summer of 1988 driven by a GCM and the ECMWF analyses

Gregory S. Jenkins^{a,*}, Eric J. Barron^b

^a Department of Meteorology, Pennsylvania State University, 503 Walker Building, University Park, PA, 16802, USA

^b Earth System Science Center, Pennsylvania State University, University Park, PA, 16802, USA

Received 15 October 1998; accepted 25 March 1999

Abstract

A regional climate model is driven at its lateral boundaries by the European Center for Medium Range Forecast (ECMWF) analyses and the GENESIS global climate model (GCM) during the spring and summer of 1988. Observed sea surface temperatures (SSTs) are imposed as boundary conditions in the GCM. The regional climate simulations are integrated from April 1, 1988 through September 1, 1988 using a horizontal grid spacing of 108 km over the continental United States. The largest differences in both the atmospheric circulation and the surface climate of the regional climate simulations with GCM boundary conditions occur during June of 1988 when compared to the analyses or observations. The primary cause for the different results in the regional climate simulations is the lack of an anomalous upper level circulation in the GCM. In summary, the regional model does not add additional value to the large-scale patterns, which show the same systematic bias as the GCM. However, precipitation in the regional model is closer to observations when compared to the GCM. This implies that the use of an ensemble average to provide boundary conditions in conjunction with improved physics of the regional model may enhance the regional detail that is absent in low resolution GCMs. © 2000 Elsevier Science B.V. All rights reserved.

Keywords: regional climate simulation; ECMWF; GCM; climate variability; regional climate models; 1988 summer drought

1. Introduction

Tropical atmospheric forcing associated with El Niño and La Niña events can serve as a source for anomalous weather in the United States. El Niño events are often associated with anomalous winter

season weather, while La Niña events can influence both anomalous winter and summer season weather. To capture or predict the extra-tropic circulation associated with external tropical variability in global climate models (GCMs), numerous ensemble members are averaged together. GCM simulations using the ensemble approach exhibit forecast skill for the extra-tropics when sea surface temperature (SST) anomalies are specified (Shukla, 1998). However, in many fully coupled atmosphere–ocean climate models the amplitude of SST anomalies in the central

* Corresponding author. Tel.: +1-814-865-0479; fax: +1-814-865-3663.

E-mail address: osei@essc.psu.edu (G.S. Jenkins).

Pacific are underestimated (Meehl and Arblaster, 1998). Consequently, the ocean and atmospheric variability associated with most elevated greenhouse gas simulations could be underestimated. This is especially true for North America, since SST anomalies in the tropical Pacific can strongly influence seasonal conditions at the surface and throughout the troposphere.

The summer of 1988 produced drought conditions that affected much of the continental United States. The most intense period of drought and above normal temperatures occurred in June of 1988, but the conditions leading up to the spring–summer drought were in place during March (Namias, 1991). Significant losses occurred in the agricultural sector during the summer drought. The total economic losses were estimated at 39 billion for the U.S. during the summer of 1988 (Kogan, 1995). The drought of 1988 appeared concurrently with a cold SST anomalies in the eastern and central Pacific and has been linked with the La Niña event of 1988 (Trenberth and Branstator, 1988; Trenberth and Branstator, 1992; Trenberth and Guillemot, 1996). It is also possible that there were surface–atmosphere feedbacks which may have perpetuated the drought of 1988 (Olgesby and Erickson, 1989; Atlas et al. 1993).

Chen and Newman (1998) have examined the 1988 summer drought on shorter time-scale and found that the two upper-level anti-cyclones, one at the beginning of June and the other at the end of June were responsible for the mean monthly conditions. Further, they demonstrate that anomalous outgoing longwave radiation (OLR) patterns occurred in the western Pacific just prior to the development of the anomalous upper level anti-cyclones over North America. Further, the observations show anomalous upper level anticyclones that first appear over Southeast Asia, then the in central North Pacific within 1 week to the appearance of an anticyclonic circulation over North America. Hence, it is possible that the eastward propagation of Rossby waves forced by anomalous heating associated anomalous OLR was the source of the anti-cyclonic circulation over North America. Together, atmospheric forcing from the western Pacific, the evolving La Niña event and surface-atmosphere feedbacks may have served as primary or secondary causes for the summer drought of 1988.

Several studies have examined the summer drought of 1988 with regional climate models (Giorgi et al., 1996; Hong and Leetmaa, 1998). Giorgi et al. (1996) used the regional climate model version 2 (RegCM2) driven at the boundaries by the European Center for Medium Range Forecast (ECMWF) analyses during the summer of 1988 over the western and central U.S. to evaluate the RegCM2's ability to capture seasonal variability during extreme conditions. They also examined the effects of soil moisture on precipitation processes, surface sensible heat and latent heat fluxes. Hong and Leetmaa (1998) used the National Center for Environmental Prediction (NCEP) Regional Spectral Model (RSM) over lower 48 United States in the model domain to simulate the summer of 1988 at 50 km horizontal grid spacing.

In this paper we examine the summer drought of 1988 using a regional climate model (RegCM2) which is driven at the lateral boundaries by the ECMWF analyses during the spring and summer of 1988. A primary objective of this simulation is to evaluate the RegCM2's ability to represent the regional aspects of precipitation, surface climate and the large-scale circulation (200-mb zonal winds and 500-mb geopotential heights) in comparison to the ECMWF analyses and observations during the drought conditions. In addition, we examine the regional climate simulations for the time period (spring) leading up to the summer drought conditions in 1988.

A second objective of this paper is the use of boundary conditions from a GCM to drive the RegCM2 during an extreme event. Recently, Risbey and Stone (1996) addressed and evaluated the use of GCM output for regional climate assessment. They compared various GCMs (Community climate model Version 1 and 2, NASA's Goddard Institute for Space Studies (GISS) model) at various model resolutions against observations on various time scales (10-year average, dry and wet winters, composites of large storm events) during the 1980s with emphasis on the Sacramento Basin. The authors note a number of important findings including: (a) the lack of variability in GCM dynamic fields during observed wet and dry periods; (b) a weakness in the GCM representation of strong storms which affected the Sacramento basin; (c) an improvement in the simulated

west coast precipitation but marginal improvements in the simulations of the stationary wave pattern and jet streams at high spectral resolutions (T106). By introducing the second regional simulation, the internal errors (associated with model physics) can be isolated from errors associated with lateral boundary conditions.

Recently, a regional climate model study was undertaken over Europe with the lateral boundaries being forced by observations and a GCM to isolate the source of systematic errors during a 10-year period (Nogeur et al., 1998). Their findings include (a) that lateral boundary conditions account for most of the error for upper troposphere winds (60–80% — total error variance) and mean sea level pressure (> 80% — total error variance) throughout the year. (b) Boundary conditions can serve as a source of error for moisture variables including precipitation. This can occur as a result of an excessive supply of moisture at the boundaries. (c) Internal regional climate model physics are associated with errors in the simulation of cloud amounts. (d) Sometimes, the internal regional climate models errors compensate for the boundary errors. In this study, we isolate the sources of systematic error similar to Nogeur et al. (1998) but on seasonal time-scales during a period when the tropical SSTs in the eastern Pacific are cooler than normal.

It can be argued that one GCM-regional climate model simulation is insufficient to capture an event driven by external tropical variability from the central and eastern Pacific. The suggested approach would be to produce an ensemble average from numerous GCM simulations to drive the regional climate model (Kumar and Hoerling, 1995; Trenberth et al., 1998). However, there are several difficulties associated with this approach: (1) the computational costs are very high; (2) an ensemble average from various ensemble members may smear out important synoptic features at the boundaries.

In summary, the objectives of this paper are: (1) to quantify the differences between the ECMWF analyses and a regional climate model simulation when it is driven at the lateral boundaries by ECMWF analyses during the spring/summer of 1988. (2) To quantify the differences between the ECMWF analyses and a regional climate model simulation when it is driven at the lateral boundaries by a GCM during

the spring/summer of 1988. (3) To compare monthly surface energy fluxes of the regional climate model simulations of (1) and (2). In Section 2, we describe the GCM, regional climate model and set of experiments for this study. In Section 3, the results are presented with the discussion and conclusion in Section 4.

The first objective of this paper has been examined by Giorgi et al. (1996) and Hong and Leetmaa (1998) but with a finer grid-point spacing than the model simulations reported here. There have also been numerous studies examining a GCM ability or inability to accurately simulate the mid-latitude responses to externally variability especially during the winter season (Trenberth and Branstator, 1992; Kumar et al., 1996; Hoerling and Kumar, 1997). However, there have been few studies to date that quantitatively examine the response of regional climate model when forced at the boundaries by a GCM that use tropical SST anomalies as boundary conditions.

2. Model description and experiments

GENESIS V 1.02 (Thompson and Pollard, 1995) is a hybrid of the National Center for Atmospheric Research (NCAR) Community Climate Model (CCM). GENESIS is a global spectral model written in terrain-following sigma coordinates and has a horizontal resolution of approximately 4.5° of latitude by 7.5° of longitude when computed on a rhomboidal 15 Gaussian grid (R15). GENESIS has 12 vertical levels with the three lowest model levels representing the planetary boundary layer (PBL). The model incorporates full radiative transfer calculations (delta Eddington approximation) and has an interactive cloud scheme. Convection is treated using an explicit sub-grid buoyant plume model and water vapor is advected in grid-space by the semi-Lagrangian method. GENESIS uses a land-surface package (LSX) for computing the energy and moisture fluxes between the biosphere and the atmosphere on a $2^\circ \times 2^\circ$ horizontal grid. LSX includes two vegetation layers (canopy and sub-canopy), and multiple soil and snow layers.

GENESIS has been integrated for a 10-year period using observed SSTs from January 1, 1979 through December 31, 1988. In this paper, however,

the focus is on the period from April 1, 1988 through September 1, 1988. The large-scale climate fields (horizontal motions and geopotential height fields) from the GENESIS GCM are compared with the R15 gridded ECMWF analyses (Trenberth, 1992) to assess GCM capability to simulate the large-scale flow. In addition, model simulated precipitation is compared to the observed precipitation amounts from the Global Precipitation Climatology Project (GPCP) data set which are reconstructed from station and satellite sources at a resolution of $2.5^\circ \times 2.5^\circ$ (Huffman et al., 1997). The observed temperatures are obtained from the $5^\circ \times 5^\circ$ global data set of Jones (1994) and observed cloud fractions are obtained from the International Satellite Cloud Climatology Project (ISCCP) data set (Hurrell and Campbell, 1992).

The regional climate model which is driven at the lateral boundaries by the GENESIS GCM and ECMWF analyses is referred to as RegCM2 and is described by Giorgi et al. (1993a,b). In the simulations driven by GENESIS and the ECMWF analyses, there are 14 sigma levels and the top of the model is 80 mb. The Kuo cumulus parameterization used here is similar to Jenkins and Barron (1997).

The RegCM2 uses the Biosphere–Atmosphere Transfer Scheme (BATS) for computing the fluxes of heat, moisture and momentum between the atmosphere and surface (Dickinson et al., 1993; Giorgi et al., 1993a). There is a three-layer soil water model in RegCM2 that is comprised of a 10-cm thick surface soil layer, a 1-m thick root zone and a 5-m thick deep soil layer.

ECMWF analyses and GENESIS meteorological fields are used to update the lateral boundaries of the RegCM2 at 12 h intervals. The technique consists of the relaxation method described by Anthes et al. (1987). The method employs a Newtonian and a diffusion term applied to the outermost four grid point rows of the domain, whose effect is to smoothly drive the model meteorological fields (wind components, temperature, humidity and surface pressure fields) near the boundaries (toward the time-dependent boundary) (Davies and Turner, 1977). Linear relaxation is applied at the boundaries.

The RegCM2 simulation driven by the ECMWF analyses is denoted as RegECM and the RegCM2 simulation driven by GENESIS is denoted as the

RegGEN. The domain in the simulations includes all of the 48 lower United States, parts of northern Mexico and southern Canada. The eastern Pacific, western Atlantic, and the Gulf of Mexico are also included in the domain. A horizontal grid spacing of 108 km is assumed in these simulations. The center of the grid is 40°N , 95°W , and there are 34 north–south grid points and 60 east–west grid points. Both simulations are initialized at 0000 UTC, April 1, 1988 and integrated through 0000 UTC, September 1, 1988.

3. Results

3.1. Large-scale circulation

Fig. 1 shows the time-averaged 500-mb heights during April–May (AM), June and July–August (JA) for the ECMWF analyses. The most notable feature during this period is an amplified 500-mb ridge during June that is displaced eastward of the AM position. During June, the ridge is located over the Great Plains and troughs can be found along the eastern and western U.S. seaboard, respectively. During JA there is a collapse of the 500-mb ridge with a nearly zonal geopotential height pattern over the United States.

Figs. 2–4 show the 500-mb height differences between the GENESIS, RegGEN and RegECM simulations and the ECMWF analyses for the three time periods. Fig. 5 shows the 500-mb height differences between the RegGEN and RegECM simulations. Over the continental United States, both the GENESIS and RegGEN simulations show the largest differences during the month of June (Figs. 2 and 3). The largest negative differences are found over the Midwest near 90°W because a simulated 500-mb ridge does not evolve during June (not shown). The negative geopotential height bias is reflected in Table 1 for the RegGEN simulation that shows the largest bias and RMS errors found in June.

In contrast to the RegGEN simulation, the simulated RegECM ridge is found over the central United States during June but the 500-mb geopotential heights are 20–30 m higher than the ECMWF analyses over the Great Plains (Fig. 4b). The positive bias in geopotential heights continues into JA for the

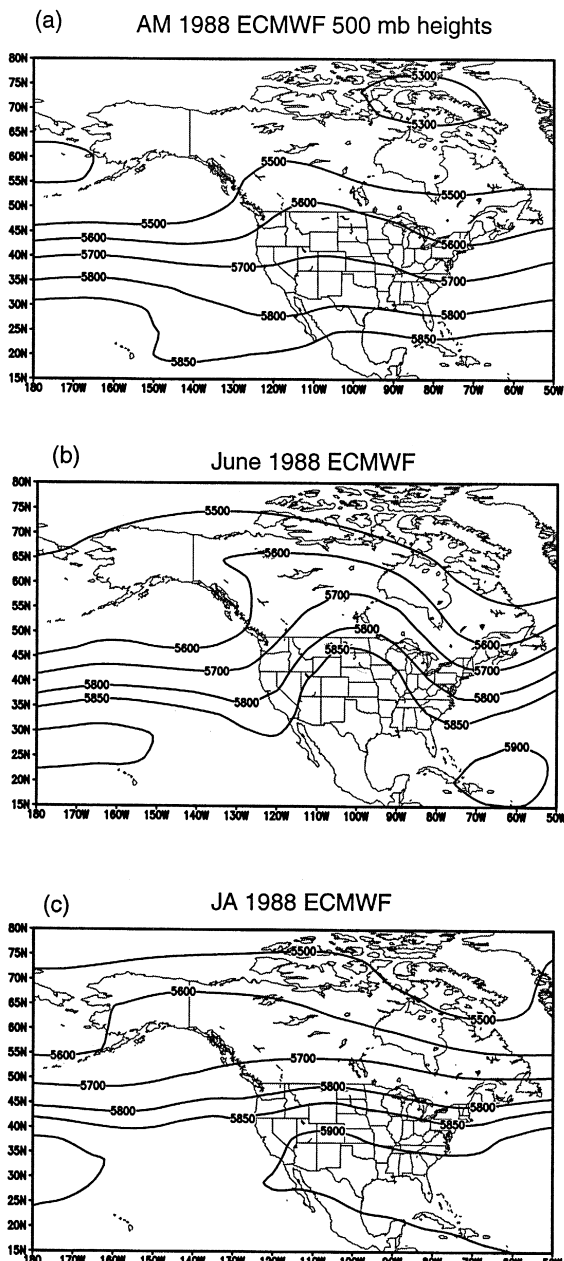
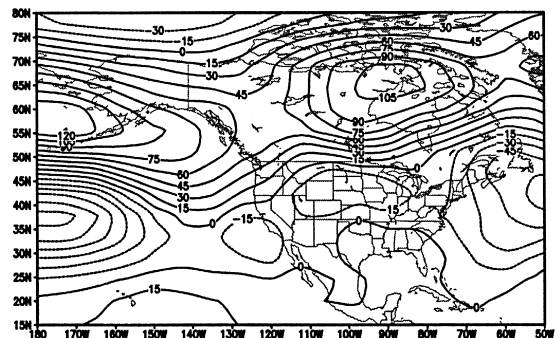


Fig. 1. 500-mb geopotential height for the ECMWF analyses . (a) AM; (b) June; (c) JA.

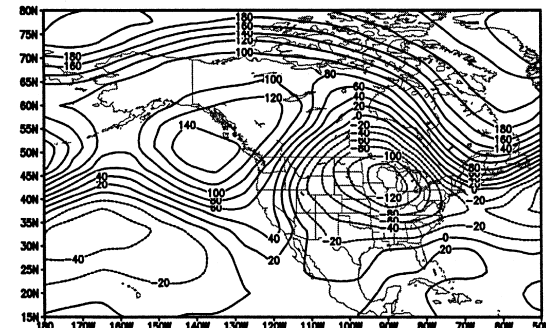
RegECM simulation (Fig. 4c, Table 2). Fig. 5a–c shows the differences during the three periods between the RegGEN and RegECM simulations. Here we find similar differences to those of GENESIS and ECMWF analyses (Fig. 2) and RegGEN and

ECMWF analyses (Fig. 3) when comparing RegGEN to the RegECM simulation (Fig. 5). The geopotential heights are more than 160 m lower in the RegGEN simulation than the RegECM simulation during June of 1988. The results imply that boundary conditions are primarily responsible for differences in the regional climate simulations.

(a) GENESIS Minus ECMWF AM 1988 500 mb Heights



(b) GENESIS Minus ECMWF June 1988 500 mb Heights



(c) GENESIS Minus ECMWF JA 1988 500 mb Heights

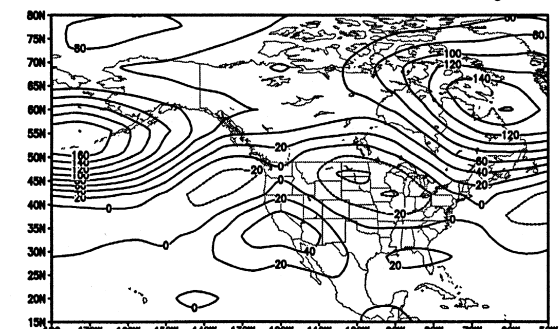


Fig. 2. 500-mb geopotential heights differences (GENESIS minus ECMWF). (a) AM ; (b) June; (c) JA. Units in meters.

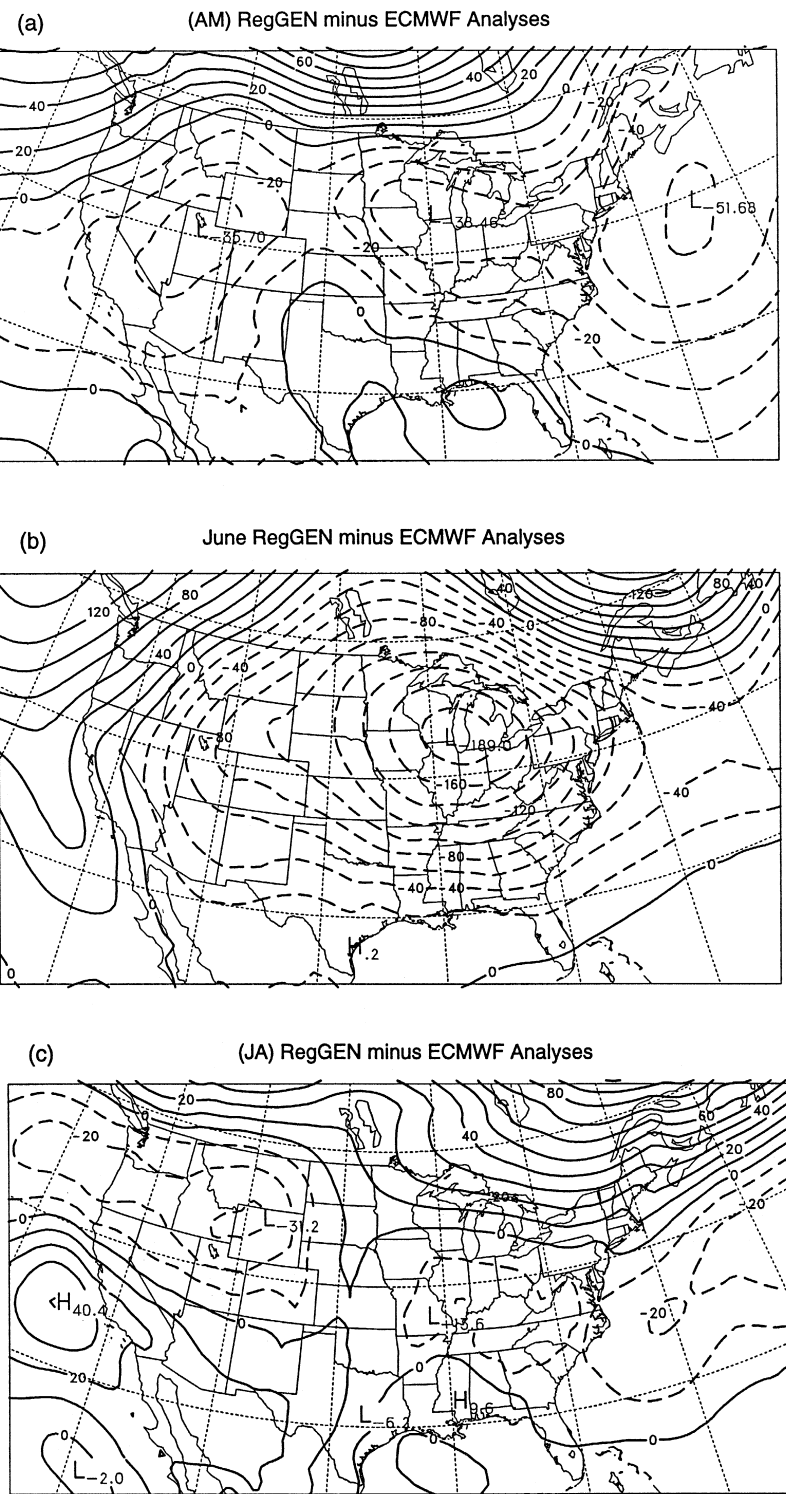


Fig. 3. 500-mb geopotential heights differences (RegGEN minus ECMWF). (a) AM ; (b) June; (c) JA. Units in meters.

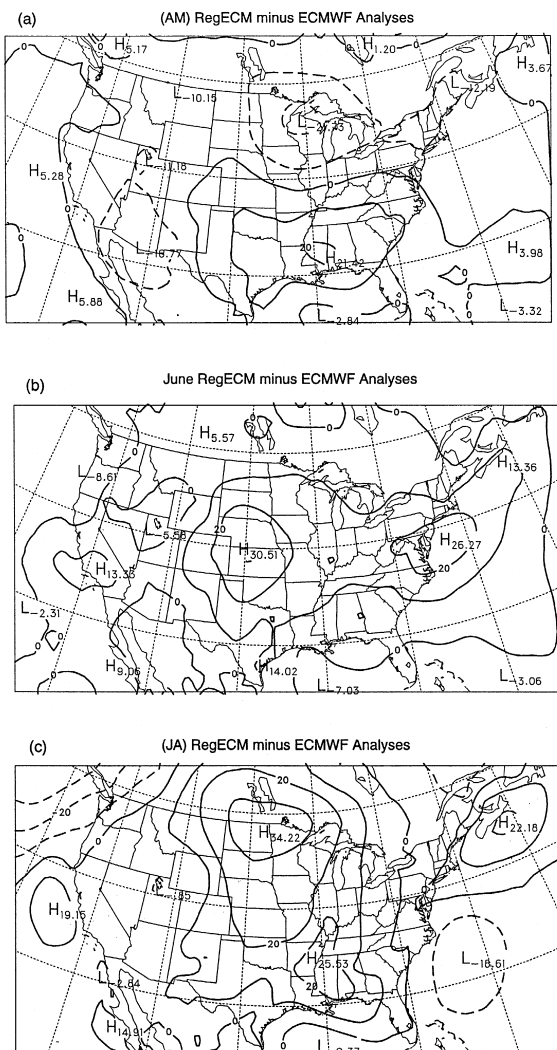


Fig. 4. 500-mb geopotential heights differences (RegECM minus ECMWF). (a) AM ; (b) June; (c) JA. Units in meters.

Tables 1 and 2 show larger biases and RMS errors are found in the RegGEN simulations for 200-mb winds, especially during June and JA. The positive zonal wind bias and RMS error in the RegGEN simulations during June is caused by a simulated Jet Stream that is found near 35°N compared to 55°N in the ECMWF analyses. The reduction in the JA RegGEN bias and RMS error is associated with the collapse of the upper-level ridge and the return to near zonal flow. There is an increase in the zonal wind bias and RMS error in the RegECM simulation

resulting from zonal winds that are stronger than the ECMWF analyses from Mexico to Florida (not shown). A similar pattern of wind bias is found in the RegGEN simulation relative to the ECMWF analyses. The source of these errors may be related to changes in the thermal structure at the surface and upward through the middle troposphere.

For both the RegGEN and RegECM simulations a dry bias in the PBL occurs, especially during the latter portions of the simulations. Both moisture

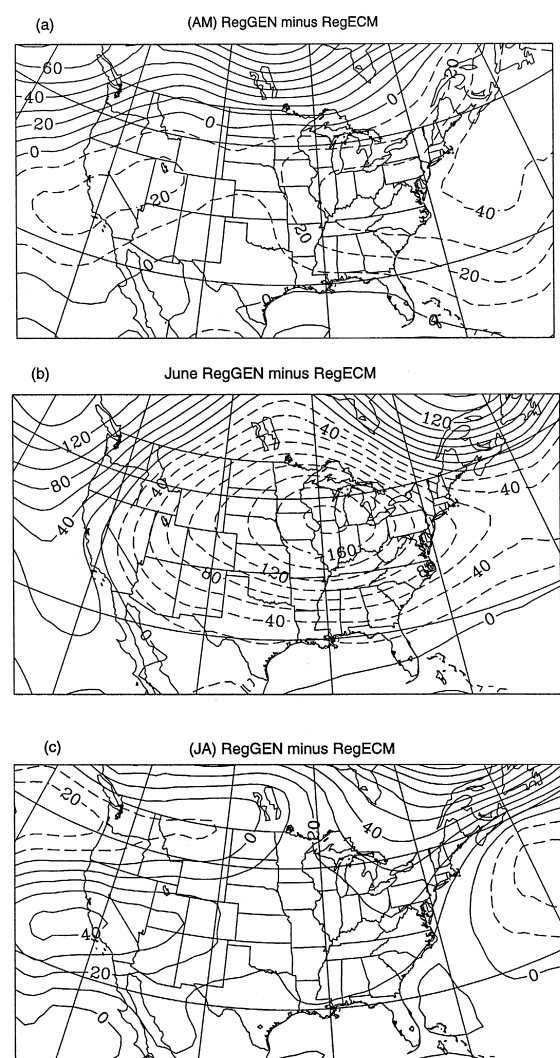


Fig. 5. 500-mb geopotential heights differences (RegGEN minus RegECM). (a) AM ; (b) June; (c) JA. Units in meters.

Table 1

Monthly biases and RMS errors for the RegGEN simulation for the entire domain

Variable	AM RegGEN	June RegGEN	JA RegGEN
850-mb moisture bias (g/kg)	-0.00813	-1.38	-1.66
850-mb RMS moisture error (g/kg)	0.0884	2.37	2.43
500-mb heights bias (m)	8.66	-20.6	5.75
500-mb RMS height error (m)	27.5	72.4	23.1
200-mb Zonal wind bias (m/s)	1.34	2.60	0.147
200-mb RMS zonal wind error (m/s)	4.94	13.6	6.18

biases and RMS errors are larger in the RegECM simulations for each of the three time periods. Land areas in the domain are the primarily source of the dry bias during each month. In the RegECM simulation, the monthly 850 mb moisture bias over land jumps from -1 g/kg during May to -2.5 g/kg in June with the onset of the anomalous 500 mb anticyclone. The moisture bias then persist for the rest of the period, with the largest moisture bias of -2.85 g/kg over land found during July. In the RegGEN simulation, there is an increase in the moisture bias in June at 850-mb over land. The monthly 850-mb moisture bias over land increases from -1.2 g/kg during July to -2.5 g/kg in August. The source of error is most likely due to the PBL scheme that excessively transports water vapor from the lower troposphere into the mid-troposphere. This feature has been noted in Giorgi et al. (1993a) and Jenkins and Barron (1997).

To understand why there are significant errors at the boundaries of the RegGEN simulation, the GENESIS simulated anomalous conditions of the tropical central and eastern Pacific are examined. Fig. 6a shows the SST anomalies during June of 1988 when compared to the mean decade of 1979–1988. Broad areas of negative SST anomalies exist near 120°W at

the Equator. However, to the west of 130°W and poleward of 10°N , positive SST anomalies are found. The observed OLR anomalies during June show positive OLR anomalies along the equator in response to negative SST anomalies (Fig. 6b). Negative SST anomalies are found to stretch from west to east in the latitude range of $8\text{--}12^{\circ}\text{N}$. In the GENESIS simulation, positive OLR values are found along the equator except for the region between 120°W and 90°W where negative OLR anomalies are found. There is no evidence of a west-to-east band of negative OLR anomalies near 10°N in the GENESIS simulation. Further, the anomalous stationary wave train in the ECMWF analyses during June 1988 (Fig. 7a) is not apparent in the GENESIS simulation (Fig. 7b). In fact, the sign of the anomalous geopotential heights are nearly of opposite signs those of the ECMWF analyses from the eastern Pacific through the Midwest. The Discrepancies in the OLR implies that precipitation over the region of anomalous SSTs is not simulated properly in the model suggesting an incorrect response in the parameterized convection. The coarse GCM resolution might smear out the amplitude or position of the SST anomaly pattern causing an improper response in the convective parameterization.

Table 2

Monthly biases and RMS errors for the RegECM simulation for the entire domain

Variable	AM RegECM	June RegECM	JA RegECM
850-mb moisture bias (g/kg)	-0.517	-1.63	-2.0
850-mb RMS moisture error (g/kg)	0.828	2.06	2.48
500-mb heights bias (m)	-1.48	4.57	4.53
500-mb RMS height error (m)	7.34	9.09	13.5
200-mb Zonal wind bias (m/s)	-0.172	0.339	0.821
200-mb RMS zonal wind error (m/s)	1.41	1.46	5.08

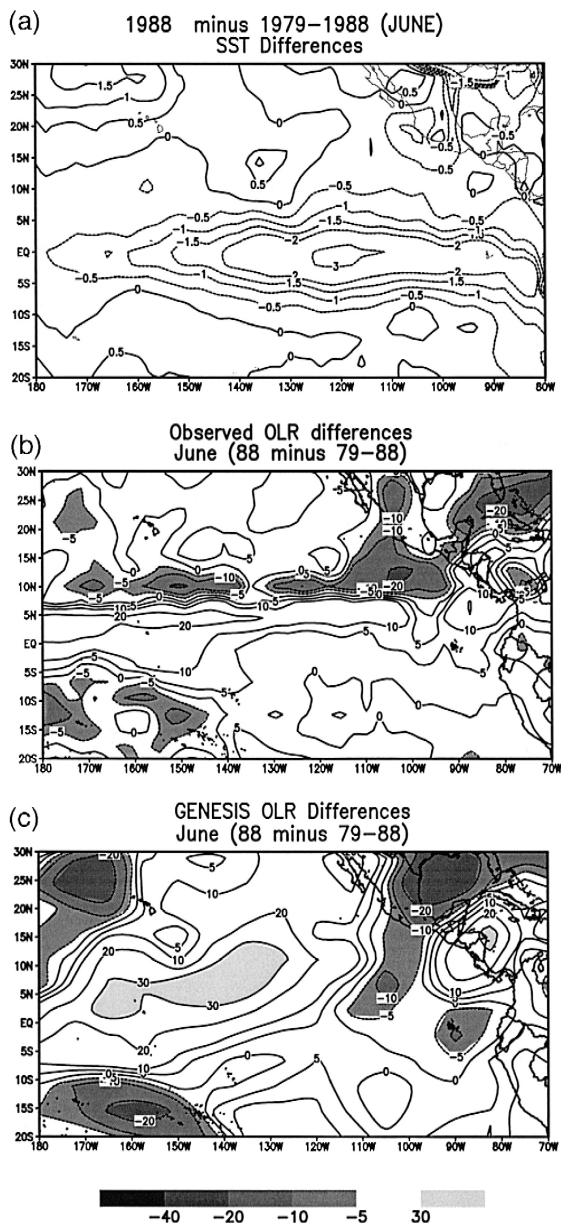


Fig. 6. June 1988 anomalies (1988 minus 1979–1988). (a) AMIP Sea Surface Temperature ($^{\circ}$ C); (b) Observed outgoing longwave radiation (OLR) [$\text{W}\cdot\text{m}^{-2}$]; (c) GENESIS OLR [$\text{W}\cdot\text{m}^{-2}$].

3.2. Precipitation, surface temperature and clouds

Figs. 8–10 show the AM, June and JA observed precipitation rates and simulated precipitation rates

of GENESIS, RegGEN and the RegECM. During each period, the GENESIS simulated precipitation is overestimated over the United States and there is no evidence of drought conditions in June (Figs. 8b–10b). While the RegGEN simulation shows a reduction in precipitation rates when compared to GENESIS, the observed precipitation pattern and variability is not captured (Figs. 8c–10c). In the RegGEN simulation the western U.S. is dry throughout each period, while the eastern U.S. remains relatively wet.

In the RegECM simulation, the AM and JA precipitation rates shows similarities to the observed precipitation, except that the precipitation rates are consistently underestimated in the Southern United States (Figs. 8d and 10d). In contrast to the RegGEN simulation, the RegECM severely underestimates precipitation rates with most of the country receiving less than 1 mm/day of rainfall (Fig. 9d). The lowest

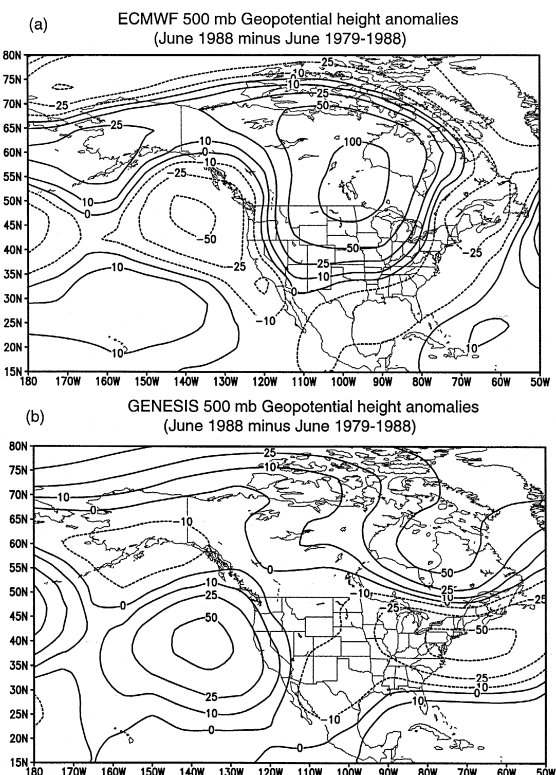


Fig. 7. 500-mb geopotential height anomalies for June 1988 (June 1988 minus June 1979–1988). (a) ECMWF analyses; (b) GENESIS. Units in meters.

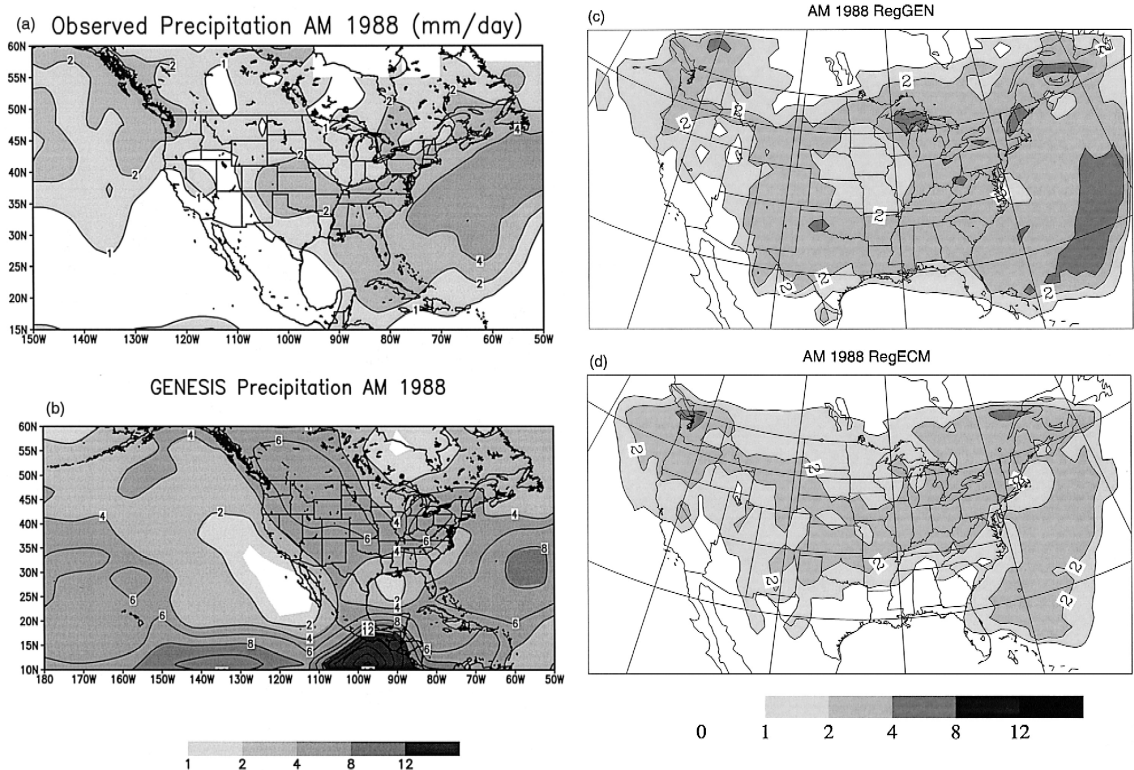


Fig. 8. April–May (AM) 1988 time-averaged precipitation. (a) Observed; (b) GENESIS; (c) RegGEN; (d) RegECM. Units in mm day^{-1} .

rainfall rates are located near the center of the 500-mb ridge while wetter conditions appear upstream and downstream of the upper-level ridge. The wetter conditions upstream of the ridge were also found in Giorgi et al. (1996) over the Rockies. During their simulation of the summer of 1988 drought, Giorgi et al. (1996) found increases in precipitation rates at some locations because larger values of sensible heat increase atmospheric instability and convection. We find large increases in sensible heat in the RegECM simulation during June 1988 (see below), but we do not find increases in precipitation rates. With the collapse of the upper-level ridge, there is a return to higher precipitation rates over much of the U.S. in the RegECM simulation, except over the Southern United States.

In June, the warmest observed temperatures are found over the Central and Southern Plains (Fig. 11a). The warmest temperatures ($> 305 \text{ K}$) are lo-

cated near the axis of the 500-mb ridge in the ECMWF analyses (Fig. 1b). In the GENESIS simulation, the warmest temperatures are located east of the Southern Plains (Fig. 11b). A tongue of warm temperatures greater than 295 K extends into southern Canada but is located to the east of the observed tongue of warm temperatures. Warmer than observed temperatures occur near California and the Great Basin in the GENESIS simulation, while cooler than observed temperatures occur over the northeastern U.S.

In the RegGEN simulations, the warmest temperatures extend from the Southern Plains northward into southern Canada. Warm temperatures greater than 300 K are confined to the Southern Plains (Fig. 11c). The observed hot temperatures over the Southern and Central plains are not simulated. Warmer than observed temperatures occur along the West Coast and near the Great Basin and cooler than observed

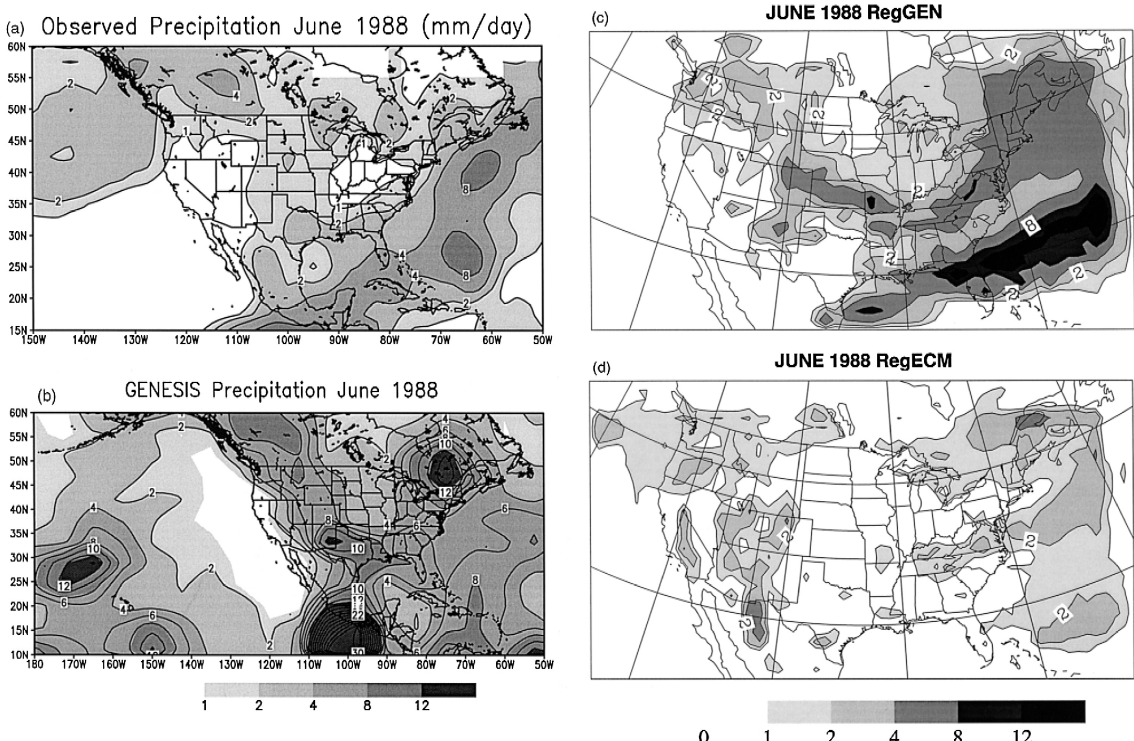


Fig. 9. June 1988 time-averaged precipitation. (a) Observed; (b) GENESIS; (c) RegGEN; (d) RegECM. Units in mm day^{-1} .

temperatures occur in the northeast U.S. similar to the GENESIS simulation. In the RegECM simulation, all of the Plains, much of the Midwest and southeast U.S. have temperatures above 302 K (Fig. 11d). The warmest temperatures are found in the Central and Southern Plains where June temperatures exceed 306 K. Thus, RegECM overestimates air temperatures over much of the Central U.S., California and the Great Basin when compared to observations.

Fig. 12 shows the total cloud fraction over the U.S. during the summer of 1988. The ISCCP data shows cloud percentages between 40% and 60% over most of the United States. The exception is the Great Basin which have cloud percentages between 20% and 40% and northeast U.S. which has 60% to 80% cloud cover (Fig. 12a). In the GENESIS simulation smaller cloud fraction is found over most of the U.S. except the eastern 1/4 of the United States and the Northern Rockies. Over the rest of the United States cloud amounts are between 20% and 40%. A

similar cloud pattern to that of GENESIS is found in the RegGEN simulation (Fig. 12c). The eastern 1/4 of the country has cloud fraction between 40% and 60% while higher values are found in the northeast United States. The high cloud fractions in the GENESIS and RegGEN simulations over the northeast are connected to a deep trough (Fig. 2b). The total cloud fractions are even lower in the RegECM simulation during the summer of 1988 (Fig. 12d). Cloud percentages greater than 80% cannot be found at any location within the United States. Cloud fractions are very low over the Great Basin, the Southern Great Plains and the Northern Rockies. These low cloud fractions are in response to the anomalous upper level circulation during June are partially responsible to the higher than observed air temperatures (Fig. 11). During June the total cloud fraction is less than 20% over much of the Midwest and Great Plains (not shown) and is suggested from the RegECM precipitation amounts during June (Fig. 12d). Further, the persistent warm bias in the RegGEN and

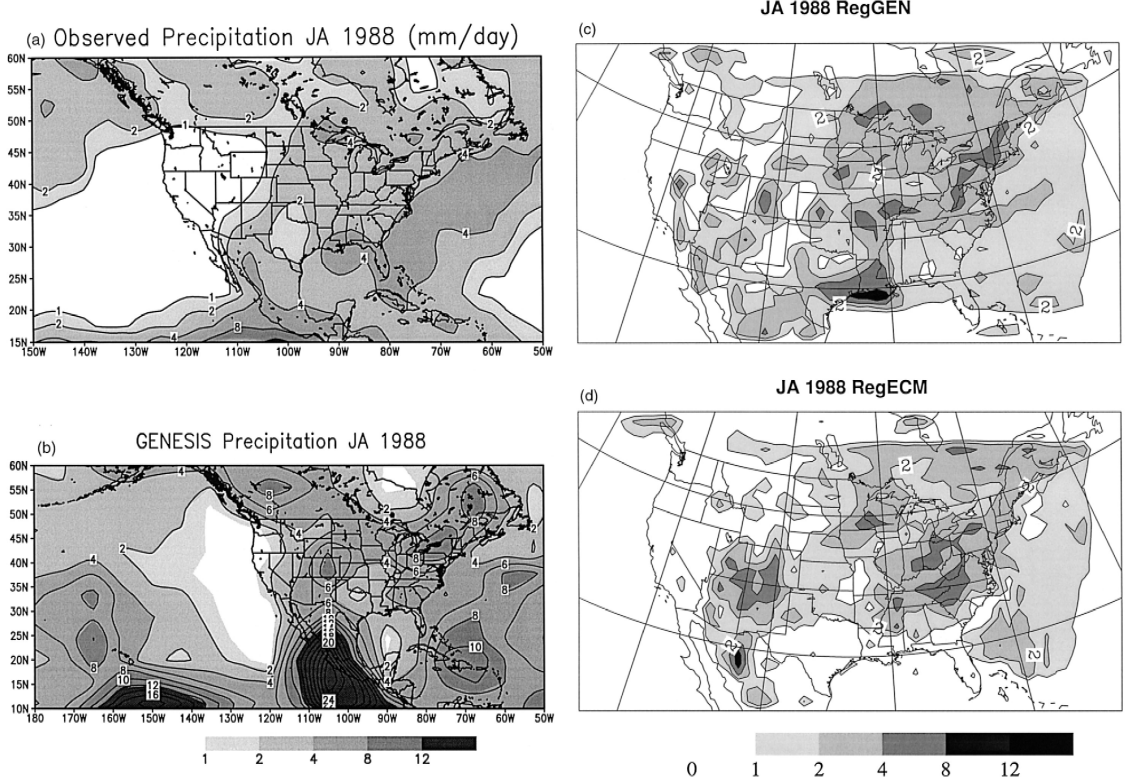


Fig. 10. July–August (JA) 1988 time-averaged precipitation. (a) Observed; (b) GENESIS; (c) RegGEN; (d) RegECM. Units in mm day^{-1} .

RegECM simulations over California and the Great Basins is due to the total cloud fraction in these regions being less than 20% during JA.

3.3. Regional surface energy budgets

In this section surface energy fluxes and soil moisture are examined over four regions in the RegECM and RegGEN simulations. The regions are the Northern Great Plains ($37\text{--}48^\circ\text{N}$, $91\text{--}105^\circ\text{W}$), the Southern Great Plains ($27\text{--}37^\circ\text{N}$, $91\text{--}105^\circ\text{W}$), the Midwest ($37\text{--}48^\circ\text{N}$, $81\text{--}91^\circ\text{W}$) and the Northeast ($37\text{--}48^\circ\text{N}$, $81\text{--}91^\circ\text{W}$). Only land points are used in the analysis of the fluxes below.

In Fig. 13, the area-averaged monthly solar radiation absorbed at the surface and total cloud fraction for the four regions is shown. In each of the regions in the RegECM simulation the highest absorbed solar radiation and lowest total cloud fractions are

found during the month of June (Fig. 13). The absorbed solar radiation monotonically increases through the late spring into the early summer due to seasonal changes in insolation. However, the upper level ridge which occupied much of the central United States during June of 1988 is responsible for a reduction in clouds and precipitation resulting in more solar radiation reaching the surface.

Overall, there are more clouds and less absorbed solar radiation in the RegGEN simulation when compared to RegECM from April through July in the four regions. In the month of August, the absorbed solar radiation is higher and the cloud fractions are lower in the RegGEN simulation in the four regions. There is no response in either absorbed solar radiation or clouds during the month of June in the RegGEN simulation except over the Southern Great Plains (Fig. 13c). There is more solar radiation being absorbed at the surface and smaller cloud fractions in

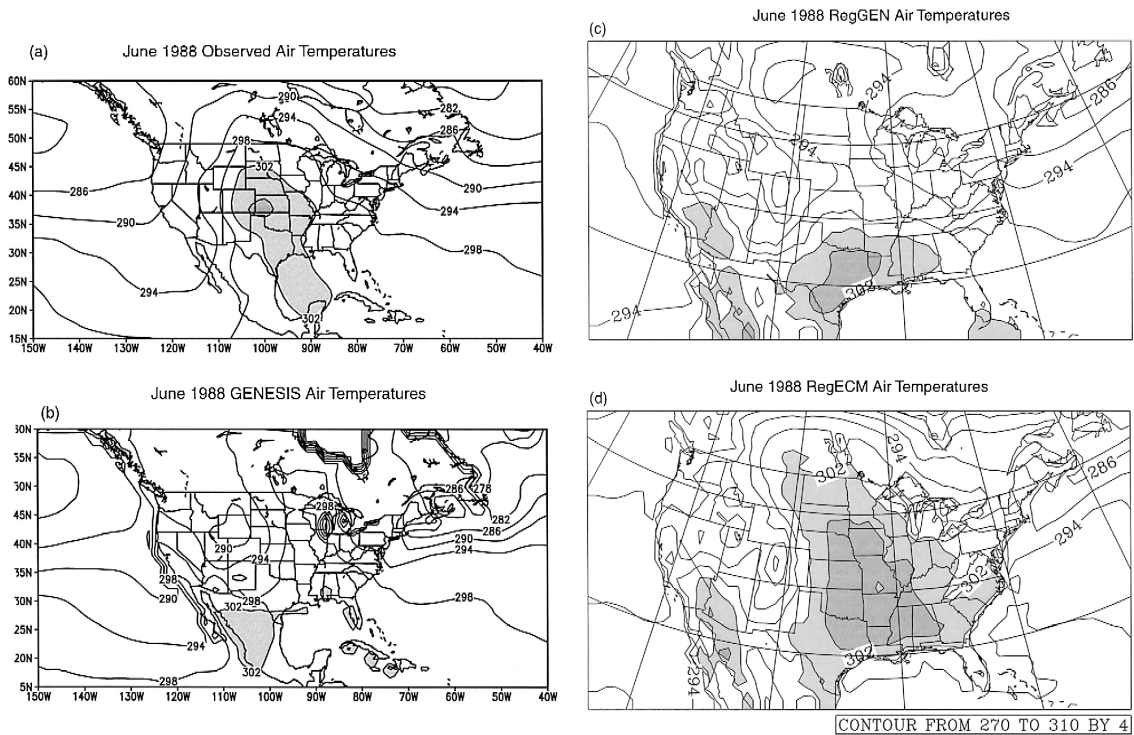


Fig. 11. June 1988 time-averaged 2-m air temperatures. (a) Observed; (b) GENESIS; (c) RegGEN; (d) RegECM. Units in kelvin. Shaded areas > 302 K.

the RegECM simulations when averaged over the four regions (Tables 3 and 4). This result is magnified during June where the absorbed solar radiation is $76 \text{ W}\cdot\text{m}^{-2}$ larger in the RegECM simulation when averaged over the four regions. Further, a total cloud fraction of 19% occurs in the RegECM simulation is computed compared to cloud fraction of 39% for the RegGEN simulation. These factors lead to 7°C warmer temperatures in the RegECM when compared to the RegGEN simulation during June (Tables 3 and 4).

Fig. 14 shows the evolution of the ratio of monthly averaged soil moisture values to the initial (April 1, 1988) soil moisture values. The soil moisture represents the moisture content in the top 50 mm of soil in the RegECM and RegGEN simulations. Both simulations show a drying of the upper soil layer in the transition from the spring through late summer season. In the RegECM simulation, the ratio falls to its lowest values in three of the four regions during

the month of June. In all regions during the month of June, the soil moisture is less than 50% of the original value on April 1. Low soil moisture ratios are found from May through July in the Southern Plains (Fig. 14b) with the lowest values found in July. In the RegGEN simulation, the lowest soil moisture ratio is found during August in each region. A dip in the June soil moisture is found over the Midwest, Northern and Southern Plains, similar to the RegECM simulation, but the lowest values are found in August. The area average over the four regions show that soils are wetter in the RegGEN simulation, with a difference of 6 mm of water in the top 50 mm of soil during the month of June (Tables 3 and 4).

Fig. 15 shows the latent heat flux during the spring and summer periods of 1988. In the case of latent heat, the RegECM simulation shows a reduction in latent heat flux during May and June and a rebound in July and August in the Northern Great

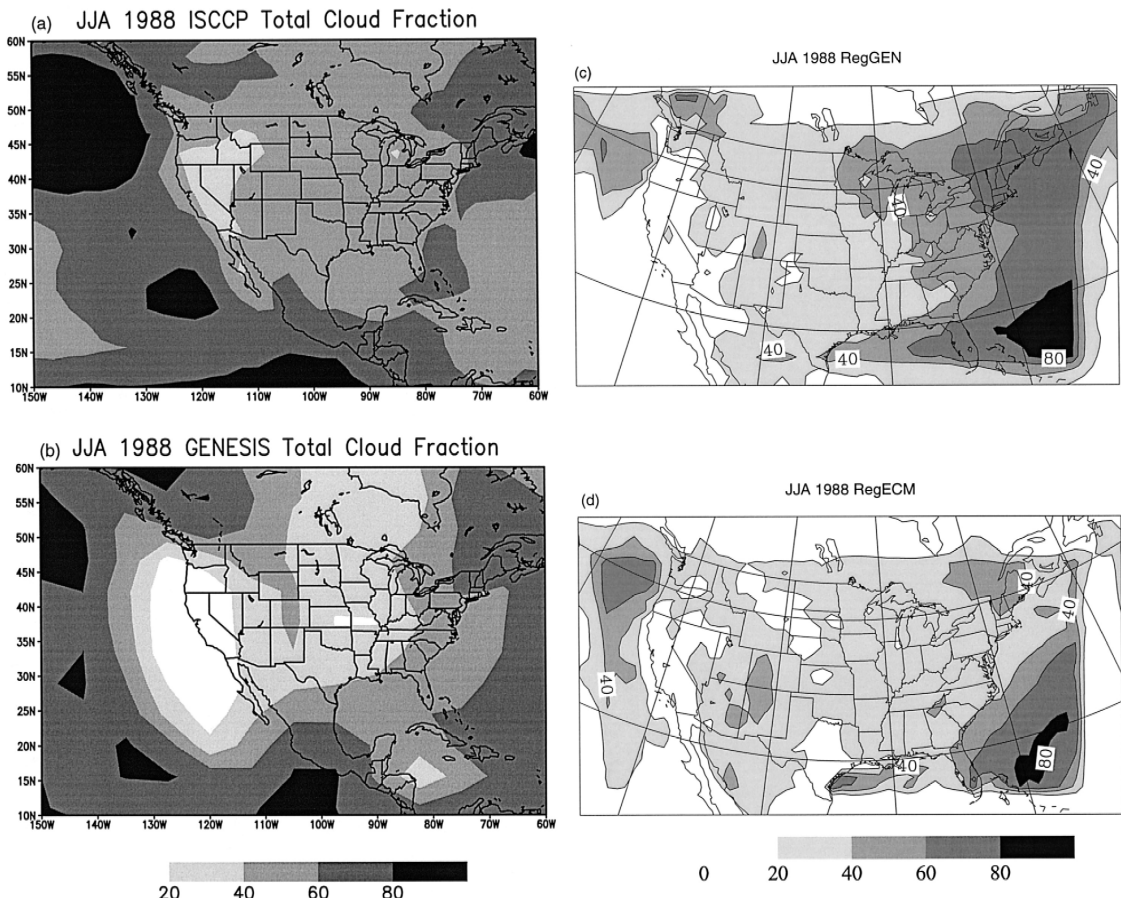


Fig. 12. Total cloud percentage during JJA of 1988. (a) Satellite-derived (ISCCP); (b) GENESIS; (c) RegGEN; (d) RegECM. Unit is percent.

Plains and the Midwest regions. Over the Southern Great Plains, the latent heat flux reaches a minimum in July and rises in August. Over the Northeast, the latent heat takes on a zigzag pattern, with low values in April, June and August and higher values in May and July (Fig. 15). In the RegGEN simulation, the lowest latent heat values are found in the month of August except in the Northeast. When averaged over all four regions, the latent heat in the RegECM simulation is lower during May, June and July when compared to the RegGEN simulation (Tables 3 and 4). The latent heat flux is approximately 18 W-m^{-2} lower during the month of June in the RegECM simulation.

The sensible heat flux in the RegECM simulation has its highest values during the month of June over

all four regions followed by lower values during JA (Fig. 16). In the RegGEN simulation, lower values of sensible heat can be found in all four regions when compared to the RegECM simulation except during the month of August over the Northern Great Plains and Midwest regions. Large differences in the sensible heat exist between the RegECM and RegGEN simulation when averaged over the four regions. During June the sensible heat flux in the RegECM simulation is nearly 43 W-m^{-2} larger than in the RegGEN simulation (Tables 3 and 4).

The large increase in sensible heat flux associated with the upper level ridge in the RegECM simulation leads to high Bowen ratios, which exceed 2 over all four regions during June (not shown). In the Southern Great Plains, a Bowen ratio greater than 2 persist

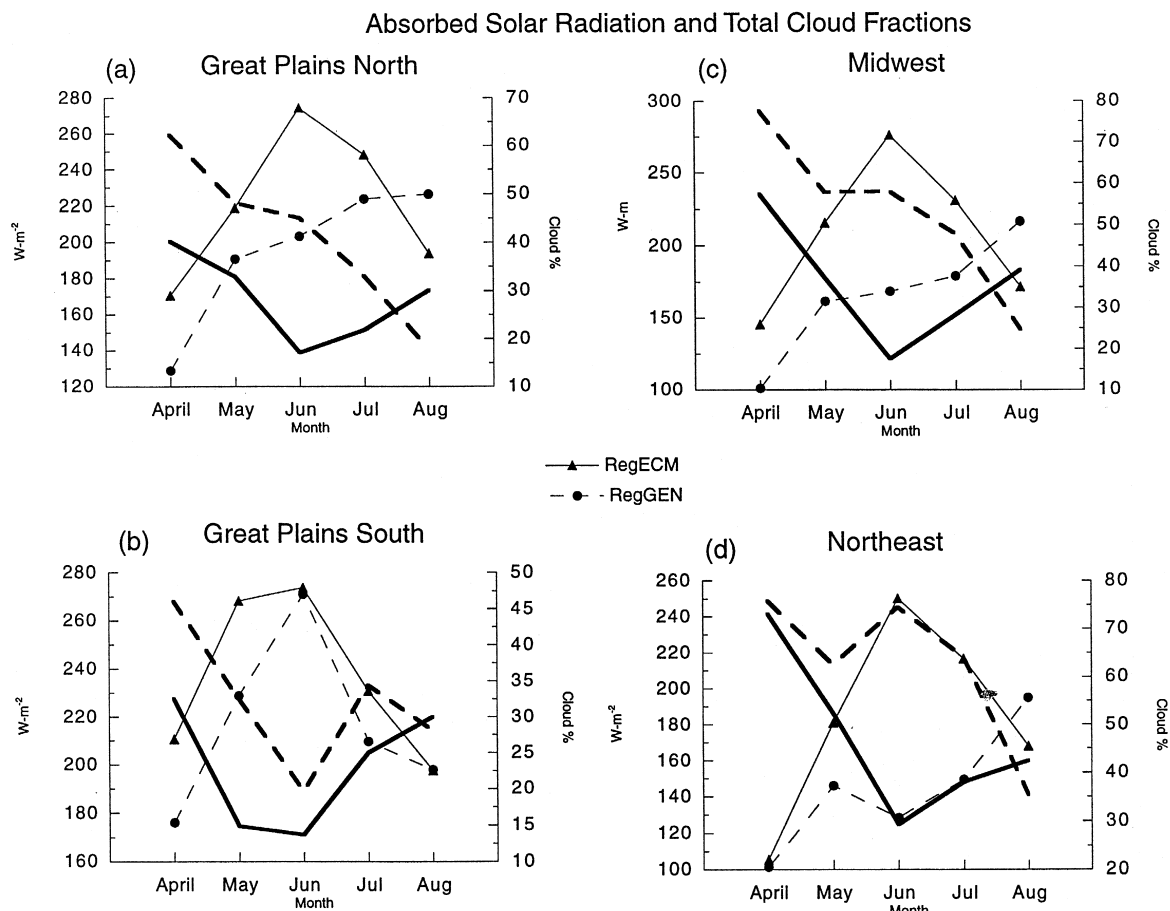


Fig. 13. Area-averaged monthly absorbed solar radiation at the surface (left vertical axis) and total cloud fraction (right vertical axis). (a) Northern Great Plains; (b) Southern Great Plains; (c) Midwest; (d) Northeast. Heavy solid and dashed lines represent the total cloud fraction; light solid and dashed lines represent the absorbed solar radiation. Solid lines is the RegECM simulation and dashed lines the RegGEN simulation.

for May, June and July. The Bowen ratio in the RegECM simulations falls below 1 during July and

August as precipitation returns to these regions, except for the Southern Great Plains. The Bowen ratio,

Table 3
Monthly values for the four regions in the RegECM simulation

Month	TS2 (K)	Cloud (fraction)	Absorbed Solar (W·m ⁻²)	Sensible heat (W·m ⁻²)	Latent heat (W·m ⁻²)	Bowen ratio (fraction)	Soil wetness (mm)
April	282.97	50.763	158.10	20.126	61.640	0.32445	26.629
May	292.77	34.316	220.90	43.017	60.037	0.90818	20.268
June	302.14	19.366	268.65	82.362	42.120	2.0215	15.079
July	303.51	28.240	231.64	61.569	55.709	1.3449	17.142
Aug	300.43	35.388	182.84	38.649	56.307	0.78974	18.942

Table 4

Monthly values for the four regions in the RegGEN simulation

Month	TS2 (K)	Cloud fraction (%)	Absorbed solar (W·m ⁻²)	Sensible heat (W·m ⁻²)	Latent heat (W·m ⁻²)	Bowen ratio (fraction)	Soil wetness (mm)
April	281.67	50.064	126.78	12.182	54.713	0.21031	28.466
May	290.94	38.707	181.82	27.912	66.880	0.43576	23.704
June	294.89	38.770	192.75	39.471	60.782	0.69978	21.393
July	299.47	37.533	190.50	34.321	74.095	0.49409	21.901
Aug	303.96	23.306	208.97	47.651	49.881	1.0977	16.740

latent and sensible heat values in the RegECM simulation are in line with the dry run simulation of Giorgi et al. (1996). The Bowen ratio in the RegGEN simulation is greater than 1 over the Southern Great

Plains from June through August. A simulated Bowen ratio greater than 1 is found over the Northern Great Plains during the month of August. When averaged over the four regions, the Bowen ratio exceeds 1

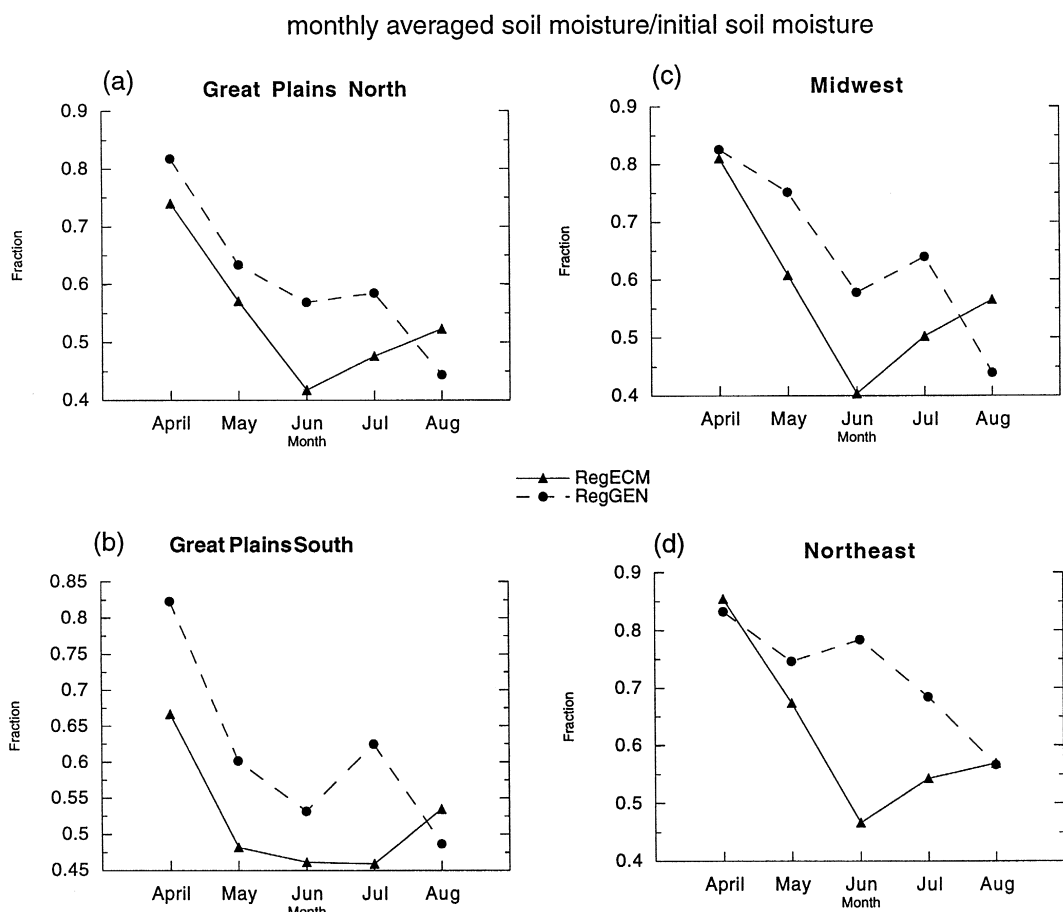


Fig. 14. Area-averaged ratio of monthly-averaged soil moisture to initial soil moisture field. (a) Northern Great Plains; (b) Southern Great Plains; (c) Midwest; (d) Northeast.

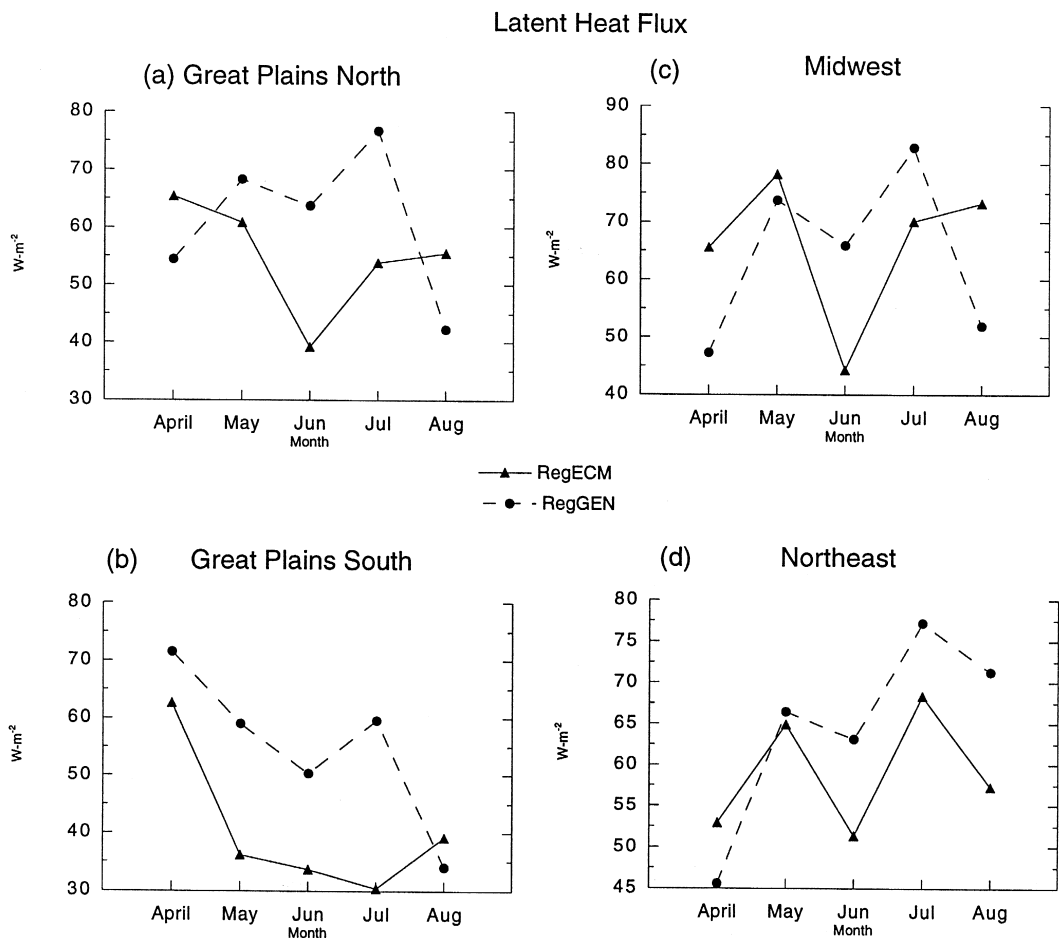


Fig. 15. Area-averaged latent heat flux. (a) Northern Great Plains; (b) Southern Great Plains; (c) Midwest; (d) Northeast. Units in $\text{W}\cdot\text{m}^{-2}$. Solid lines is the RegECM simulation and dashed lines the RegGEN simulation.

during June and July in the RegECM simulation and exceeds 1 during August in the RegGEN simulation (Tables 3 and 4).

4. Summary and conclusion

In this paper, spring and summer circulation of 1988 in the ECMWF analyses was compared to the GENESIS GCM and regional climate model simulations. In the regional climate model simulations, one simulation used the ECMWF analyses to provide lateral boundary conditions (RegECM), while in the other simulation the GENESIS GCM provided lateral boundary conditions (RegGEN).

- In summary, we found that GENESIS did not reproduce conditions at the peak of the summer drought (June) for the large-scale circulation fields. This was due in part to deficiencies in capturing atmospheric response to sea surface temperature anomalies in the central and eastern Pacific. In particular, GENESIS did not simulate the OLR anomalies in the tropics, the upper-level ridge over the central U.S., or the poleward displacement of the jet stream into southern Canada. Larger precipitation rates than the observations were found over the U.S. during most of the spring and summer periods in the GENESIS GCM.

- The errors in the GENESIS simulation of the spring-summer period of 1988 were reflected in the

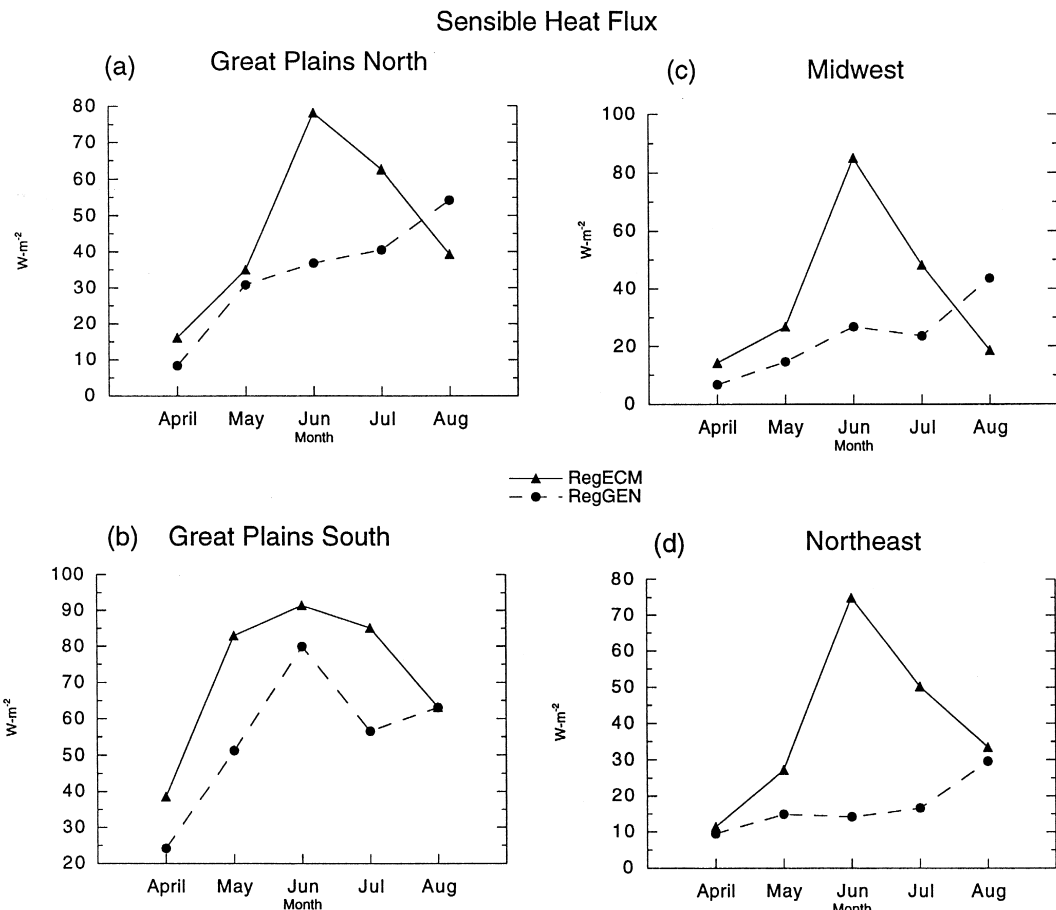


Fig. 16. Area-averaged sensible heat flux. (a) Northern Great Plains; (b) Southern Great Plains; (c) Midwest; (d) Northeast. Units in $\text{W}\cdot\text{m}^{-2}$. Solid lines is the RegECM simulation and dashed lines the RegGEN simulation.

regional climate model simulation (RegGEN) that used GENESIS lateral boundary conditions. This was particularly true for the dynamic components of the atmosphere, where large biases and RMS errors were found during June of 1988. The regional climate model simulation did, however, reduce the precipitation rates when compared to GENESIS. The precipitation pattern in the RegGEN simulation is poorly represented when compared to observations. These findings are consistent to those of Noguer et al. (1998).

In the regional climate model simulation in which the ECMWF analyses provided the lateral boundary conditions, the large-scale circulation is well produced at the peak of the drought. Relatively

small biases and RMS errors in the large-scale circulation occurred during the spring and summer of 1988. The largest error is associated with the simulated precipitation rates, which were considerably lower at the peak of the drought than the observations.

- Hot temperatures occurred during June of 1988 in the regional climate model simulation (RegECM) driven by the ECMWF analyses. The temperatures remained very warm during July and August in the simulation in agreement with the observations. The surface temperatures in the RegECM simulation were, however, warmer than the observed temperatures in part to lower than observed cloud fractions in response to the anomalous upper-level circulation.

The low cloud fraction increased the amount of solar radiation absorbed at the surface, raising surface temperatures.

- Soil moisture, latent heat and cloud amounts were reduced in response to the anomalous upper-level circulation and warmer surface temperatures in the RegECM simulation. A reduction in soil moisture is in agreement with the reduction in soil moisture measured in Illinois (Kunkel, 1989). These results are also in agreement with the low vegetation condition index (VCI) associated with the drought that were found over a large portion of the U.S. east of the Rockies during June and July (Kogan, 1995). Absorbed solar radiation at the surface, sensible and the Bowen ratio where increased in response to atmospheric conditions especially during June of 1988. The Bowen ratio was greater than 2 for the four regions analyzed during June in response to the elevation of sensible heat and the reduction of latent heat. The values were larger than the measured values of Kunkel (1989) in Illinois were a Bowen ratio greater than 1 was found during the first half of July.

- As a consequence of GENESIS not capturing the anomalous upper-level circulation during June, large differences in the surface energy fluxes between the RegGEN and RegECM simulations occur. When averaging over the Great Plains, Midwest and Northeast, the absorbed solar radiation and sensible and fluxes are 75 and 43 W·m⁻² smaller in the RegGEN simulation when compared to the RegECM simulation. The latent heat flux in the RegGEN simulation is 18 W·m⁻² higher than in the RegECM simulation. These sizable differences occur while temperatures are 7°C cooler in the RegGEN simulation than the RegECM simulation.

- The results from these simulations reflect the concerns of Rigsby and Stone (1996) and more recently that of Warner et al. (1997) and Noguer et al. (1998) demonstrating how errors in the stationary wave pattern can lead to systematic errors at the regional scale. The results clearly point to the need of GCMs to properly simulate the stationary wave pattern thereby providing reasonable boundary conditions for regional climate model simulations. While this aspect is critical for extreme conditions such as the drought of 1988, it is also important for understanding regional patterns of possible future climate

change due to elevated atmospheric greenhouse gases. The stationary wave pattern may be altered with elevated greenhouse gas concentrations. In addition, anomalous warming and cooling of the tropical pacific SSTs (El Niño and La Niña events) are expected to continue, thereby altering perhaps a different mean stationary wave pattern imposed by elevated greenhouse gas concentrations.

- When the ECMWF analyses was used to force the RegCM2, we still find errors in the zonal wind and geopotential height fields, but these errors are small when compared to the RegGEN simulation. The largest differences between the RegECM and observations are for the simulated precipitation. The relatively coarse domain along with the non-explicit physics for the cumulus parameterization used in this study are likely responsible for precipitation differences. Because the Kuo cumulus parameterization is dependent on moisture convergence, during periods of weak forcing (summer season) and under extreme conditions such as June of 1988, the Kuo cumulus parameterization will under-predict rainfall. Further, because of non-explicit physics and the coarse resolution of 108 km used here, these simulations cannot resolve and/or properly simulate the smaller-scaled weather systems (thunderstorms, squall lines, MCCs), nor the physical processes (updraft, downdraft, mixed-phased precipitation) associated with these systems. While it may be possible to address some of the errors associated with the lateral boundary conditions (Warner et al., 1997), the errors associated with extreme conditions on seasonal time-scales present serious challenges to the GCM and regional climate modeling community.

Acknowledgements

This work was supported under NASA Grant # NAGW-2686: The Global Water Cycle: Extension Across Earth Sciences.

References

- Anthes, R.A., Hsie, E.Y., Kuo, Y.H., 1987. Description of the Pennsylvania State/NCAR mesoscale model version 4 (MM4), NCAR Technical Note, NCAR/TN-282 + STR, 66 pp.

- Atlas, R., Wolfson, N., Terry, J., 1993. The effect of SST and soil moisture anomalies on GLA model simulations of the 1988 U.S. summer drought. *J. Clim.* 6, 2034–2048.
- Chen, P., Newman, M., 1998. Rossby wave propagation and the rapid development of upper-level anomalous anticyclones during the 1988 U.S. drought. *J. Clim.* 11, 2491–2504.
- Davies, H.C., Turner, R.E., 1977. Updating prediction models by dynamical relaxation: an examination of the technique. *Q. J. R. Meteorol. Soc.* 103, 225–245.
- Dickinson, R.E., Kennedy, P.J., Henderson-Sellers, A., Wilson, M., 1993. Biosphere-Atmosphere Transfer Scheme (BATS) version 1e as coupled to the NCAR community climate model, NCAR Technical Note, NCAR TN-387 + STR.
- Giorgi, F., Marinucci, M.R., Bates, G.T., 1993a. Development of a second-generation regional climate model (RegCM2): Part I. Boundary-layer and radiative transfer processes. *Mon. Weather Rev.* 121, 2794–2813.
- Giorgi, F., Marinucci, M.R., Bates, G.T., 1993b. Development of a second-generation regional climate model (RegCM2): Part II. Convective processes and assimilation of lateral boundary conditions. *Mon. Weather Rev.* 121, 2814–2832.
- Giorgi, F., Mearns, L.O., Shields, C., Mayer, L., 1996. A regional model study of the importance of local versus remote controls of the 1988 drought and 1993 flood over the Central United States. *J. Clim.* 9, 1150–1168.
- Hoerling, M.P., Kumar, A., 1997. Origins of extreme climate states during the 1982–83 ENSO Winter. *J. Clim.* 10, 2859–2870.
- Hurrell, J.W., Campbell, G.G., 1992. Monthly mean global satellite data sets available in CCM history tape format, NCAR Tech. Note, NCAR/TN-371 + STR.
- Huffman, G.J., Adler, R.F., Arkin, P., Chang, A., Ferraro, R., Gruber, A., Janowiak, J., McNab, A., Rudolf, B., Cshneider, U., 1997. The global precipitation climatology project (GPCP) combined precipitation dataset. *Bull. Am. Meteorol. Soc.* 78, 5–20.
- Hong, S.Y., Leetmaa, A., 1998. An evaluation of the NCEP RSM for regional climate modeling. *J. Clim.*, In press.
- Jenkins, G.S., Barron, E.J., 1997. Global climate model and coupled regional climate model simulations over the Eastern United States: GENESIS and RegCM2 simulations. *Global Planet. Change* 15, 3–32.
- Jones, P.D., 1994. Hemispheric surface air temperature variations: a reanalysis and an update to 1993. *J. Clim.* 7, 1794–1802.
- Kogan, F.N., 1995. Drought of the late 1980s in the United States as derived from NOAA polar-orbiting satellite data. *Bull. Am. Meteorol. Soc.* 76, 655–668.
- Kumar, A., Hoerling, M.P., 1995. Prospects and limitations of seasonal atmospheric GCM prediction. *BAMS* 76, 335–345.
- Kumar, A., Hoerling, M.P., Leetmmaa, A., Sardeshmukh, P., 1996. Assessing a GCM's suitability for making seasonal prediction. *J. Clim.* 9, 115–129.
- Kunkel, K.E., 1989. A surface energy budget view of the 1988 Midwestern United States drought. *Boundary-Layer Meteorol.* 48, 217–225.
- Meehl, G.A., Arblaster, J.M., 1998. The Asian–Australian monsoon and El Niño-southern oscillation in the NCAR climate system model. *J. Clim.* 11, 1356–1385.
- Namias, J., 1991. Spring and summer 1988 drought over the contiguous United States — causes and prediction. *J. Clim.* 4, 54–65.
- Noguer, M., Jones, R., Murphy, J., 1998. Sources of systematic errors in the climatology of a regional climate model over Europe. *Clim. Dyn.* 14, 691–712.
- Oglesby, R.J., Erickson, D.J. III, 1989. Soil moisture and the persistence of North American drought. *J. Climatol.* 2, 1362–1380.
- Risbey, J.S., Stone, P.H., 1996. A case study of the adequacy of GCM simulations for input to regional climate change assessments. *J. Clim.* 9, 1441–1467.
- Shukla, J., 1998. Predictability in the midst of chaos: a scientific bias for climate forecasting. *Science* 282, 728–731.
- Thompson, S.L., Pollard, D., 1995. A global climate model (GENESIS) with a land–surface-transfer scheme (LSX): Part 1. Present climate simulations. *J. Clim.* 8, 732–761.
- Trenberth, K.E., Branstator, G.W., 1988. Origins of the 1988 North American drought. *Science* 242, 1640–1645.
- Trenberth, K.E., 1992. Global analysis from ECMWF and Atlas from 1000 to 10 mb circulation statistics, NCAR Tech. Note, NCAR/TN-373 + STR.
- Trenberth, K.E., Branstator, G.W., 1992. Issues in establishing causes of the 1988 drought over North America. *J. Clim.* 5, 159–172.
- Trenberth, K.E., Guillemot, C.J., 1996. Physical processes involved in the 1988 drought and 1993 floods in North America. *J. Clim.* 9, 1288–1298.
- Trenberth, K.E., Branstator, G.W., Karoly, D., Kumar, A., Lau, N-C., Ropelewski, C., 1998. Progress during TOGA in understanding and modeling global teleconnections associated with tropical sea surface temperatures. *JGR* 103, 14291–14324.
- Warner, T.T., Peterson, R.A., Treadon, R.E., 1997. A tutorial on lateral boundary conditions as a basic and potentially serious limitation to regional numerical weather prediction. *Bull. Am. Meteorol. Soc.* 78, 2599–2617.